We are IntechOpen,
the world's leading publisher of
Open Access books
Built by scientists, for scientists

4,800
Open access books available

122,000
International authors and editors

135M
Downloads

Our authors are among the

154
Countries delivered to

TOP 1%
most cited scientists

12.2%
Contributors from top 500 universities

BOOK
CITATION
INDEX
CLARIVATE ANALYTICS
INDEXED

WEB OF SCIENCE™

Selection of our books indexed in the Book Citation Index
in Web of Science™ Core Collection (BKCI)

Interested in publishing with us?
Contact book.department@intechopen.com

Numbers displayed above are based on latest data collected.
For more information visit www.intechopen.com

Spectral Observations of PM10 Fluctuations in the Hilbert Space

Thomas Plocoste and Rudy Calif

Abstract

During the last 20 years, many megacities have experienced air pollution leading to negative impacts on human health. In the Caribbean region, air quality is widely affected by African dust which causes several diseases, particularly, respiratory diseases. This is why it is crucial to improve the understanding of PM10 fluctuations in order to elaborate strategies and construct tools to predict dust events. A first step consists to characterize the dynamical properties of PM10 fluctuations, for instance, to highlight possible scaling in PM10 density power spectrum. For that, the scale-invariant properties of PM10 daily time series during 6 years are investigated through the theoretical Hilbert frame. Thereafter, the Hilbert spectrum in time-frequency domain is considered. The choice of theoretical frame must be relevant. A comparative analysis is also provided between the results achieved in the Hilbert and Fourier spaces.

Keywords: PM10 data, empirical mode decomposition, Hilbert spectral analysis, time-frequency representation, Fourier space

1. Introduction

Generally, the concentration of air pollutants varies and is impacted by the local pollutant emission levels and meteorological and topographical conditions [1, 2]. Particulate matter (PM) is a complex mixture of elemental and organic carbon, ammonium, nitrates, sulfates, mineral dust, trace elements, and water [3]. PM with an aerodynamic diameter of <10 µm, i.e., PM10, are well known for their impact on human health [4]. Many studies have highlighted that exposure to PM increases the number of hospital admissions for cardiovascular disease, acute bronchitis, asthma attacks, respiratory disease, and congestive heart failure [5–8]. In the Caribbean area, one of the main emitters of PM10 is from large-scale sources, i.e., African dust [9]. Knowledge of the dynamics of PM10 process is crucial to elaborate strategies and construct tools to predict dust events. The time-frequency distribution of a signal provides information about how the spectral content of a signal evolves with time, thus providing an ideal tool to dissect, analyze, and interpret nonstationary signals [10]. Contrary to classical methods, the need of a time-frequency representation (TFR) is stemmed from the inadequacy of either time domain or frequency domain analysis to fully describe the nature of nonstationary signals [10]. In literature, there are numerous methods to obtain energy density as a function of time and frequency simultaneously as the short-time Fourier transform (STFT), Hilbert-Huang transform (HHT), and wavelet transform (WT) [10–12].

In this study, the scaling properties of PM10 data are firstly analyzed, and then the TFR is investigated. In order to highlight the performance of the Hilbert space, an analysis of PM10 data was also performed in the Fourier space.

This chapter is organized as follows. Section 2 presents PM10 data analyzed in this study. Section 3 describes the methods applied in order to investigate PM10 dynamics. Section 4 comments on the results obtained and then discusses them.

2. Experimental data

Guadeloupe archipelago is a French West Indies island located in the middle of the Caribbean basin, i.e., 16.25°N latitude and 61.58°W longitude, which experiences a tropical and humid climate [13, 14]. The time series analyzed here belong to Guadeloupe air quality network which is managed by the Gwad'Air agency (http://www.gwadair.fr/). PM10 concentrations are measured at Pointe-à-Pitre (16.2422°N 61.5414°W) using the Thermo Scientific tapered element oscillating microbalance (TEOM) models 1400ab and 1400-FDMS. Hourly PM10 concentrations were sampled during the period from 1 January 2005 to 31 December 2010. We processed these data into daily average concentrations. In total, there are 2150 daily averaged data points available continuously for 6 years. **Figure 1** displays PM10 daily signal illustrating huge fluctuations and thus indicating a strong variability. These strong oscillations observed in the middle of each year are attributed to PM10 related to dust outbreaks coming from the African coast from May to September [9]. For the rest of the year, PM10 is mainly generated by anthropogenic pollution [15].
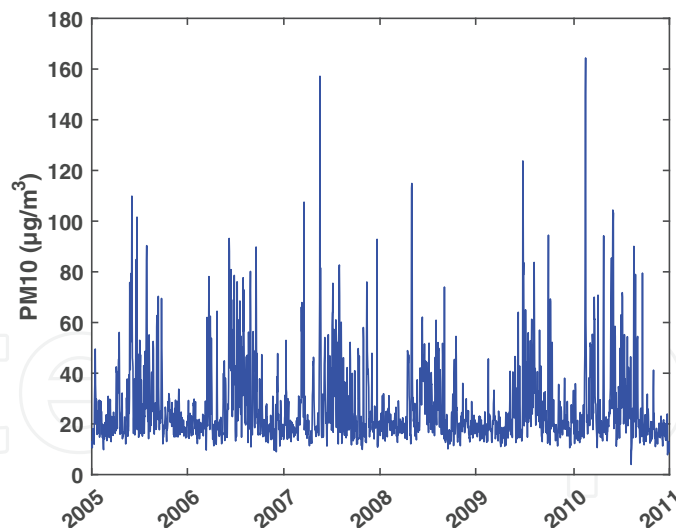
Figure 1.
Illustration of PM10 daily average concentrations between 2005 and 2010, highlighting intermittent burst events with huge fluctuations.

3. Methods

3.1 Scaling analysis (1D representation)

The description of natural phenomena by the study of statistical scale laws is not recent [16]. Self-similarity of complex systems has been widely observed in nature and is the simplest form of scale invariance. A scale invariance can be detected by

computing of power spectral density (PSD). The PSD separates and measures the amount of variability occurring in different frequency bands. In this study, PSD are estimated through the Fourier and Hilbert spaces.

3.1.1 Fourier analysis

In order to investigate the scaling properties of PM10 data, classically the discrete Fourier transform of the times series considered is computed. The expression of Fourier transform $X(f)$ for a process $x(t)$ is recalled here. An N point-long interval is used to construct the value at frequency domain point f, X_f [17]:

$$X(f) = \int_{-T}^{+T} x(t)e^{-2\pi ift} \, dt \tag{1}$$

Thus, the analytical expression of $X(f)$ is [18]

$$|X(f)| = \sqrt{\mathcal{R}e^2(X(f)) + \mathcal{I}m^2(X(f))} \tag{2}$$

Consequently the power spectral density $E(f)$ is estimated by computing the following expression:

$$E(f) = |X(f)|^2 \tag{3}$$

3.1.2 Hilbert analysis

To determine the scale invariance of a given time series in a joint amplitude-frequency space, the Hilbert-Huang transform [19, 20] is performed. HHT can be summarized in two steps: (i) empirical mode decomposition (EMD) and (ii) Hilbert spectral analysis (HSA). Empirical mode decomposition is a powerful tool to separate a nonlinear and nonstationary time series into a sum of intrinsic mode functions (IMF) without a priori basis as required by traditional Fourier-based method [19–21]. An IMF must satisfy the following two conditions: (i) the difference between the number of local extrema and the number of zero-crossings must be zero or one, and (ii) the local maxima and the envelope defined by the local minima are close to zero. Therefore, the original signal $x(t)$ is decomposed into a sum of $n1$ IMF modes with the residual $r_n(t)$:

$$x(t) = \sum_{m=1}^{n-1} C_m(t) + r_n(t) \tag{4}$$

To obtain a physically significant IMF, this selection process must be stopped by a certain criterion. For more details, EMD decomposition is widely described in the literature [19–23].

To characterize the time-frequency energy distribution from the original signal $x(t)$, HSA is applied on each obtained IMF component $C_m(t)$ to extract the instantaneous amplitude and frequency [19, 24]. The Hilbert transform is defined by:

$$\tilde{C}_m(t) = \frac{1}{\pi} P \int_{-\infty}^{+\infty} \frac{C_m(t')}{t - t'} \, dt' \tag{5}$$

with P the Cauchy principal value [24, 25]. We can specify an analytical signal z for each IMF mode $C_m(t)$ with

$$Z_m(t) = C_m(t) + j\tilde{C}_m(t) = A_m(t)e^{j\varphi_m(t)} \tag{6}$$

where $A_m(t) = |Z_m(t)| = \sqrt{C_m(t)^2 + \tilde{C}_m(t)^2}$ describes an amplitude and $\varphi_m(t) = \arg(z) = \arctan\left[\frac{\tilde{C}_m(t)}{C_m(t)}\right]$ represents the phase function of IMF modes. Consequently, the instantaneous frequency $\omega_m(t)$ is defined from the phase $\varphi_m(t)$ by

$$\omega_m(t) = \frac{1}{2\pi}\frac{d\varphi_m(t)}{dt} \tag{7}$$

Thus, the original signal $x(t)$ can be expressed as

$$x(t) = \mathcal{R}e\sum_{m=1}^{N}\mathcal{A}_m(t)e^{j\varphi_m(t)} = \mathcal{R}e\sum_{m=1}^{N}\mathcal{A}_m(t)e^{j\int_{-\infty}^{t}\omega_m(t)dt} \tag{8}$$

where $\mathcal{R}e$ is a part real [19, 20, 26].

Due to the simultaneous representation of frequency modulation and amplitude modulation, the HHT can be considered as a generalization of the Fourier transform [19, 20]. The energy in a time-frequency space is designated as the Hilbert spectrum with $H(\omega,t) = \mathcal{A}^2(\omega,t)$. The Hilbert marginal spectrum $h(\omega)$ is defined by

$$h(\omega) = \frac{1}{T}\int_{0}^{T}H(\omega,t)dt \tag{9}$$

where T is the total data length. The Hilbert spectrum $H(\omega,t)$ gives a measure of amplitude from each frequency and time, while the marginal spectrum $h(\omega)$ gives a measure of the total amplitude from each frequency [27]. As a result, the marginal spectrum can be compared to the Fourier spectrum [19, 20].

In conclusion, for a scale-invariant process, the Fourier $E(f)$ and the Hilbert $h(\omega)$ spectral densities obtained follow a power law over a range of frequencies:

$$E(f) \sim f^{-\beta_f} \tag{10}$$

$$h(\omega) \sim \omega^{-\beta_h} \tag{11}$$

where f and ω are the frequencies and β_f and β_h are the spectral exponents, respectively, in the Fourier and Hilbert spaces. It reveals the scale-free memory effect as a power law dependence of the frequency distribution. Consequently, β_f and β_h contain information about the degree of stationarity of the studied parameter [16, 28, 29]:

- If β_f or β_h <1, the process is stationary.

- If β_f or β_h >1, the process is nonstationary.

- If 1< β_f or β_h <3, the process is nonstationary with increments stationary.

- Spectral analysis has been widely applied in various research fields [30–34].

3.2 Time-frequency representation (2D representation)

3.2.1 Spectrogram

The spectrogram (SPEC) of a signal $x(t)$ is defined as the squared magnitudes of the STFT as shown in Eq. (12) [12]:

$$\mathrm{SPEC}_x(t,f) = |S_x(t,f)|^2 \tag{12}$$

where $S_x(t,f) = \int_{-\infty}^{+\infty} x(\tau)w(\tau - t)e^{-if\tau}d\tau$ is the STFT of $x(t)$, $w(\tau)$ is a window (e.g., Hanning, rectangular, Hamming), t is time, and f is frequency.

As depicted in Eq. (13), SPEC roughly describes the energy density of the signal at point (t,f) [12]:

$$\int_{-\infty}^{+\infty} \int_{-\infty}^{+\infty} \mathrm{SPEC}_x(t,f)\mathrm{dtdf} = \int_{-\infty}^{+\infty} |x(t)|^2\mathrm{dt} \tag{13}$$

The SPEC has been applied successfully in various research fields [12, 35–37]. The main advantages of SPEC are an easily understanding interpretation, and it allows a fast computation. However, the main drawback of SPEC is the same as that of the STFT [12]. Indeed, there is a trade-off between time and frequency resolution.
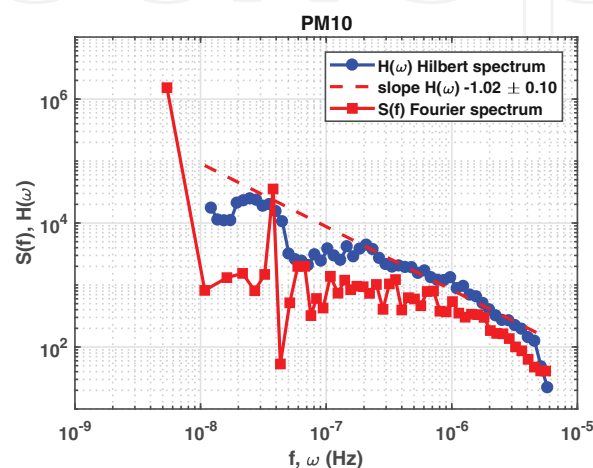
3.2.2 Hilbert spectrum

The Hilbert spectrum (HS) is a joint time-frequency representation introduced by [19]. It is important to notice that the two important tools (i.e., EMD and HS) for exploratory analysis of the data are provided by HSA method. This approach was applied successfully in various research fields as fault diagnosis for rolling bearing [11], turbulence [38], environment [34, 39], and geophysics [40], to cite a few.

4. Results

4.1 Scaling properties

In order to identify the presence of scaling in PM10 time series, the PSD is estimated in the Hilbert and Fourier spaces. **Figure 2** depicts the power spectral density provided by the Hilbert transform and the Fourier transform. On this figure, we try to detect a power law behavior of the form $h(\omega) \sim \omega^{-\beta_h}$ and $E(f) \sim f^{-\beta_f}$ where β_h and β_f are, respectively, the spectral exponents in the Hilbert and Fourier spaces. On the frequency range $2.09 \times 10^{-7} \leqslant f \leqslant 4.57 \times 10^{-5}$ Hz which corresponds to time scales 6.1 hours$\leqslant T \leqslant 55.4$ days, a power law behavior is clearly

Figure 2.
The spectrum of PM10 time series in the Hilbert space and the Fourier space. A power law behavior is significant only in the Hilbert space.
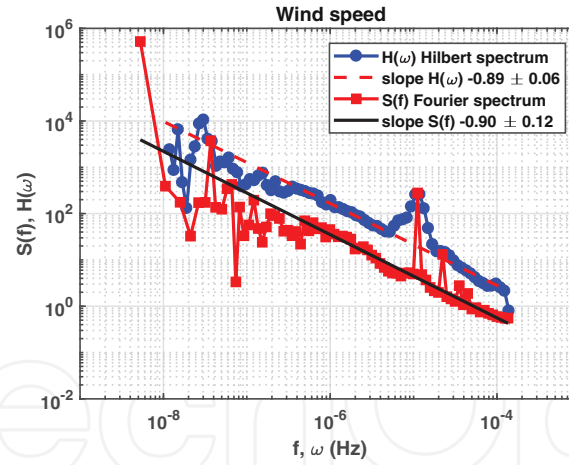
Figure 3.
The spectrum of wind speed in the Hilbert space and the Fourier space. A power law behavior is observed in both spaces.

noticed in the Hilbert space with an estimated spectral exponent $\beta_h = 1.02 \pm 0.10$. β_h is equal to 1 power law scaling observed in the mesoscale range [41]. In the Fourier space, this power law is not significant. This is due to the existence of intermittent dust events with huge fluctuations in PM10 data (see **Figure 1**). Indeed, the Fourier transform is a linear asymptotic approach which requires high-order harmonic components to mimic nonlinear and nonstationary process [42]. Thus, the high-order harmonics may lead an artificial energy transfer flux from a large scale (low frequency) to a small scale (high frequency) in the Fourier space. Consequently, the Fourier-based spectrum may be contaminated by this artificial energy flux [42]. The artificial energy transfer may give a less steep power spectrum as we observed in **Figure 2**. By contrast, combined with the EMD method, HSA has very local abilities both in physical and spectral domains and does not require any higher-order harmonic components to simulate the nonlinear and nonstationary events. As a consequence, HSA method may provide a more accurate scaling exponent and singularity spectrum [42].

According to [43], wind speed dominates the amount of pollutant dispersion in the atmospheric boundary layer. In addition, this meteorological parameter could also transport PM10 from large-scale sources, i.e., African dust [9]. To complete our results, we used hourly wind speed measurements provided by the French weather office (Météo France Guadeloupe) located at Abymes (16.2630°N 61.5147°W). PM10 and wind speed measurements are very close, i.e., ≈8.1 km of distance, and performed at the center of the island under the same atmospheric conditions [2]. **Figure 3** illustrates the PSD provided by the Hilbert transform and the Fourier transform for wind speed data. This time, a power law behavior is observed in both spaces on the same frequency range $3.54 \times 10^{-7} \leqslant f \leqslant 1.36 \times 10^{-4}$ Hz which corresponds to time scales 2.1 hours $\leqslant T \leqslant$ 32.7 days. Contrary to PM10 which is a passive scalar, wind speed is a vector quantity. The estimated spectral exponents are identical with, respectively, 0.89 ± 0.06 and 0.90 ± 0.12 in the Hilbert and Fourier spaces. As PM10, spectral exponent values are also close to -1. For wind speed, at low frequencies, a spectrum close to the 1 power law is likely occurs close to a rough surface, due to a strong interaction between the mean flow vorticity and the fluctuating vorticity [44, 45].

4.2 Time-frequency domain

The TFR in the Fourier and Hilbert spaces are, respectively, illustrated in **Figures 4** and **5**. Both figures show a color gradient from strong energy (in red) to

weak energy (in blue). This highlights the energy activity related to PM10 concentrations during the study period. Such an approach gives the possibility of tracking the evolution of PM10 data spectral content in time, which is typically represented by variations of the amplitudes and frequencies of the components from which the signal is composed [46].

On **Figure 4**, strong energies are observed throughout the years with slight fluctuations on the frequency range $0 \leqslant f \leqslant 1 \times 10^{-6}$ Hz. For $f > 4 \times 10^{-6}$ Hz, strong energies are also noticed in the middle of each year and at the beginning of 2010 with more fluctuations. In **Figure 5**, energy distributions are more localized. On the frequency range $0 \leqslant f \leqslant 1 \times 10^{-6}$ Hz, we can observe the influence of small-scale event on energy behavior. As noticed, this energy may be weak or null. As an example, the impact of a general strike in early 2009 that paralyzed Guadeloupean archipelago at least 2 months is highlighted by zero energy due to the lack of PM10 sources, i.e., industrial activity and road traffic. For $f > 1 \times 10^{-6}$ Hz, one can see more precisely energy variation related to dust events from mesoscale to large scale. Contrary to SPEC, HS clearly illustrates localized energy fluctuations due to small-scale event. In fact, the STFT makes an assumption that any signal as piecewise stationary and uses suitable window function to produce the short-time spectral characteristics of the signal. However, in
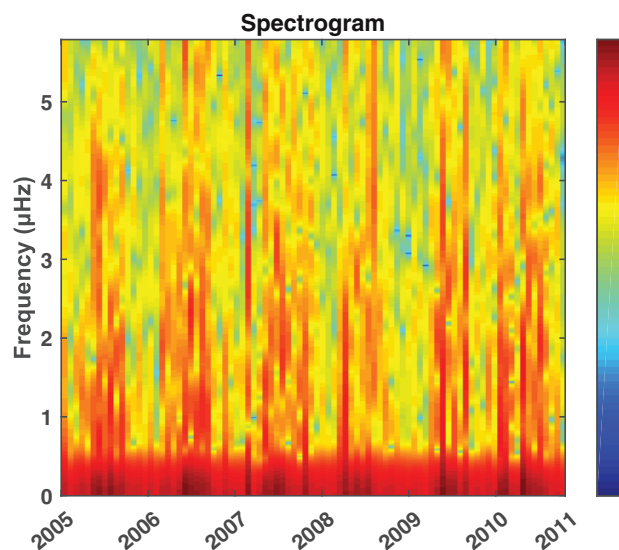
Figure 4.
Spectrogram of PM10 time series with a color gradient from strong energy (in red) to weak energy (in blue).
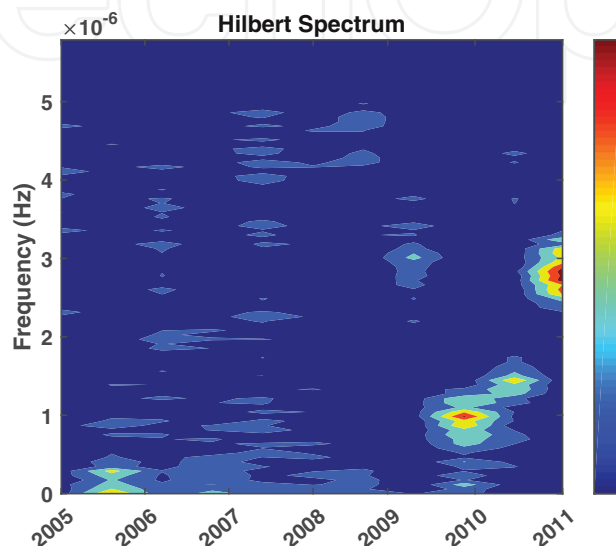
Figure 5.
Hilbert spectrum of PM10 time series with a color gradient from strong energy (in red) to weak energy (in blue).

reality, most of air pollution signals are usually nonstationary [9, 14, 47]. The Fourier transform-based technique treats the signal as a sum of predefined basis functions. If the analyzing signal is well matched with the bases, it performs better; otherwise the performance is degraded [10]. Here, the SPEC highlight energy fluctuations linked to PM10 coming from African dust between May and September (large-scale sources) [9] and from the eruption of Soufrière on Montserrat in February 2010 (mesoscale sources) [48]. However, the SPEC does not detect energy fluctuation related to anthropogenic pollution, i.e., local sources. This shows HS is a robust method in time-frequency domain. Indeed, based on the EMD method, this TFR is fully data adaptive, and the signal decomposition is performed without any predefined basis functions. These results confirm the superiority of HS over STFT in TFR.

5. Conclusion

In this paper, we investigated scaling and time-frequency properties of PM10 data in Hilbert frame. The performances obtained in the Hilbert space are compared with those achieved in the Fourier space. Firstly, with the Hilbert spectral analysis (HSA), a power law behavior is clearly observed on the frequency range $2.09 \times 10^{-7} \leqslant f \leqslant 4.57 \times 10^{-5}$ Hz which corresponds to time scales 6.1 hours $\leqslant T \leqslant 55.4$ days with an estimated spectral exponent $\beta_h = 1.02 \pm 0.10$. As HSA methodology has a very local ability in both physical and spectral spaces, the influence of intermittent dust events with huge fluctuations is included in the amplitude-frequency space which is not the case in Fourier spectrum. Thereafter, PM10 data are illustrated in time-frequency representations with the Hilbert spectrum and spectrogram. The results provide the evidence that HS-based TFR performs better than SPEC. The higher resolution in TFR offers better fluctuations of PM10 energy for $f < 1\mu$ Hz. This is due to the fact that it is impossible to increase the TF resolution at the desired level in SPEC. The major asset of HS is that the time resolution can be as precise as the sampling period and the frequency resolution depends on the choice up to the Nyquist limit. In addition, contrary to SPEC which introduces a noticeable amount of cross-spectral energy terms during the use of window function with overlapping, HS is fully adaptive to datasets due to the decomposition of the signals. These first results suggest a substantial possibility to perform a profound dynamical analysis of PM10 concentrations for the Caribbean area in order to quantify the origin and the threshold pollution.

Acknowledgements

Conflict of interest

The authors declare no conflict of interest.

Abbreviations

PM10	particulate matter with an aerodynamic diameter 10 μm or less
PSD	power spectral density
SPEC	spectrogram

EMD   empirical mode decomposition
IMF   intrinsic mode function
HSA   Hilbert spectral analysis
HHT   Hilbert-Huang transform
TFR   time-frequency representation
HS   Hilbert spectrum
STFT   short-time Fourier transform
WT   wavelet transform

Nomenclature

$E(f)$ Fourier spectral density
f frequency (Hz)
β spectral exponent
$\mathcal{A}$ instantaneous amplitude
$C(t)$ intrinsic mode function component
$h(\omega)$ Hilbert spectrum
ω instantaneous frequency (Hz)
j scale index
N total length of a sequence
$x(t)$ particulate matter signal (µg/m^3)
$r(t)$ residual of the intrinsic mode function
φ phase function of the intrinsic mode function

Author details

Thomas Plocoste[*†] and Rudy Calif[2†]

1 Department of Research in Geoscience, KaruSphère SASU, Abymes, Guadeloupe, France

2 EA 4539—LaRGE (Laboratoire de Recherche en Géosciences et Energies), Département de Physique, Université des Antilles, Pointe-à-Pitre, Guadeloupe, France

*Address all correspondence to: karusphere@gmail.com

† These authors contributed equally.

IntechOpen

References

[1] Xi W, Chen RJ, Chen BH, Kan HD. Application of statistical distribution of PM10 concentration in air quality management in 5 representative cities of China. Biomedical and Environmental Sciences. 2013;**26**(8):638-646

[2] Plocoste T, Dorville JF, Monjoly S, Jacoby-Koaly S, André M. Assessment of nitrogen oxides and ground-level ozone behavior in a dense air quality station network: Case study in the Lesser Antilles arc. Journal of the Air & Waste Management Association. 2018;**68**(12): 1278-1300

[3] Hueglin C, Gehrig R, Baltensperger U, Gysel M, Monn C, Vonmont H. Chemical characterisation of PM2.5, PM10 and coarse particles at urban, near-city and rural sites in Switzerland. Atmospheric Environment. 2005;**39**(4): 637-651

[4] Momtazan M, Geravandi S, Rastegarimehr B, Valipour A, Ranjbarzadeh A, Yari AR, et al. An investigation of particulate matter and relevant cardiovascular risks in Abadan and Khorramshahr in 2014–2016. Toxin Reviews. 2018:1-8

[5] Cairncross EK, John J, Zunckel M. A novel air pollution index based on the relative risk of daily mortality associated with short-term exposure to common air pollutants. Atmospheric Environment. 2007;**41**(38):8442-8454

[6] Kassomenos P, Papaloukas C, Petrakis M, Karakitsios S. Assessment and prediction of short term hospital admissions: The case of Athens, Greece. Atmospheric Environment. 2008; **42**(30):7078-7086

[7] Geravandi S, Sicard P, Khaniabadi YO, De Marco A, Ghomeishi A, Goudarzi G, et al. A comparative study of hospital admissions for respiratory diseases during normal and dusty days

in Iran. Environmental Science and Pollution Research. 2017;**24**(22): 18152-18159

[8] Khaniabadi YO, Fanelli R, De Marco A, Daryanoosh SM, Kloog I, Hopke PK, et al. Hospital admissions in Iran for cardiovascular and respiratory diseases attributed to the middle eastern dust storms. Environmental Science and Pollution Research. 2017;**24**(20): 16860-16868

[9] Plocoste T, Calif R, Jacoby-Koaly S. Temporal multiscaling characteristics of particulate matter PM10 and ground-level ozone O_3 concentrations in Caribbean region. Atmospheric Environment. 2017;**169**:22-35

[10] Molla MKI, Hirose K. Hilbert spectrum in time-frequency representation of audio signals considering disjoint orthogonality. Advances in Adaptive Data Analysis. 2010;**2**(03):313-336

[11] Peng Z, Peter WT, Chu F. A comparison study of improved Hilbert-Huang transform and wavelet transform: Application to fault diagnosis for rolling bearing. Mechanical Systems and Signal Processing. 2005;**19**(5): 974-988

[12] Andrade AO, Kyberd P, Nasuto SJ. The application of the Hilbert spectrum to the analysis of electromyographic signals. Information Sciences. 2008; **178**(9):2176-2193

[13] Plocoste T, Jacoby-Koaly S, Molinié J, Petit R. Evidence of the effect of an urban heat island on air quality near a landfill. Urban Climate. 2014;**10**:745-757

[14] Plocoste T, Calif R, Jacoby-Koaly S. Multi-scale time dependent correlation between synchronous measurements of ground-level ozone and meteorological parameters in the Caribbean Basin.

Atmospheric Environment. 2019;**211**: 234-246

[15] Euphrasie-Clotilde L, Molinié J, Feuillard T, Brute F. The relationship between coastal West African dust level and Caribbean island dust. WIT Transactions on Ecology and the Environment. 2017;**211**:121-127

[16] Mandelbrot B. The Fractal Geometry of Nature. New York: Freeman and Company; 1982

[17] Bracewell R. The Fourier Transform and Its Applications. 3rd ed. New York: McGraw-Hill Science; 1999

[18] Sengupta R. Interpretation of magnetic anomalies of a two-dimensional fault by Fourier integral. Canadian Journal of Exploration Geophysicists. 1975;**11**:65-71

[19] Huang NE, Shen Z, Long SR, Wu MC, Shih HH, Zheng Q, et al. The empirical mode decomposition and the Hilbert spectrum for nonlinear and non-stationary time series analysis. Proceedings of the Royal Society of London, Series A: Mathematical, Physical and Engineering Sciences. 1998;**454**(1971):903-995

[20] Huang NE, Shen Z, Long SR. A new view of nonlinear water waves: The Hilbert spectrum. Annual Review of Fluid Mechanics. 1999;**31**(1): 417-457

[21] Flandrin P, Goncalves P. Empirical mode decompositions as data-driven wavelet-like expansions. International Journal of Wavelets, Multiresolution and Information Processing. 2004; **2**(04):477-496

[22] Huang NE, Wu MLC, Long SR, Shen SS, Qu W, Gloersen P, et al. A confidence limit for the empirical mode decomposition and Hilbert spectral analysis. Proceedings of the Royal Society of London, Series A:

Mathematical, Physical and Engineering Sciences. 2003;**459**(2037):2317-2345

[23] Rilling G, Flandrin P. One or two frequencies? The empirical mode decomposition answers. IEEE Transactions on Signal Processing. 2008;**56**(1):85-95

[24] Long SR, Huang N, Tung C, Wu M, Lin R, Mollo-Christensen E, et al. The Hilbert techniques: An alternate approach for non-steady time series analysis. GRSL Geoscience and Remote Sensing Letters. 1995;**3**:6-11

[25] Cohen L. Time-Frequency Analysis. Vol. 778. New Jersey: Prentice Hall; 1995

[26] Calif R, Schmitt FG, Huang Y. Multifractal description of wind power fluctuations using arbitrary order Hilbert spectral analysis. Physica A: Statistical Mechanics and its Applications. 2013;**392**(18):4106-4120

[27] Calif R, Schmitt FG, Huang Y. The scaling properties of the turbulent wind using empirical mode decomposition and arbitrary order Hilbert spectral analysis. In: Wind Energy-Impact of Turbulence. Berlin: Springer; 2014. pp. 43-49

[28] Schertzer D, Lovejoy S. Physical modeling and analysis of rain and clouds by anisotropic scaling multiplicative processes. Journal of Geophysical Research-Atmospheres. 1987;**92**: 9693-9714

[29] Marshak A, Davis A, Cahalan R, Wiscombe W. Bounded cascade models as nonstationary multifractals. Physical Review E. 1994;**49**:55-69

[30] Windsor H, Toumi R. Scaling and persistence of UK pollution. Atmospheric Environment. 2001;**35**: 4545-4556

[31] Marr LC, Harley RA. Spectral analysis of weekday–weekend

differences in ambient ozone, nitrogen oxide, and non-methane hydrocarbon time series in California. Atmospheric Environment. 2002;**36**:2327-2335

[32] Messina AR, Vittal V. Nonlinear, non-stationary analysis of interarea oscillations via Hilbert spectral analysis. IEEE Transactions on Power Systems. 2006;**21**(3):1234-1241

[33] Choi YS, Ho CH, Chen D, Noh YH, Song CK. Spectral analysis of weekly variation in PM10 mass concentration and meteorological conditions over China. Atmospheric Environment. 2008;**42**:655-666

[34] Huang Y, Schmitt FG. Time dependent intrinsic correlation analysis of temperature and dissolved oxygen time series using empirical mode decomposition. Journal of Marine Systems. 2014;**130**:90-100

[35] Kingsbury BE, Morgan N, Greenberg S. Robust speech recognition using the modulation spectrogram. Speech Communication. 1998;**25**(1–3):117-132

[36] Sussillo D, Kundaje A, Anastassiou D. Spectrogram analysis of genomes. EURASIP Journal on Advances in Signal Processing. 2004;**2004**(1):29-42

[37] Fulop SA, Fitz K. Algorithms for computing the time-corrected instantaneous frequency (reassigned) spectrogram, with applications. The Journal of the Acoustical Society of America. 2006;**119**(1):360-371

[38] Huang Y, Schmitt FG, Lu Z, Liu Y. An amplitude-frequency study of turbulent scaling intermittency using empirical mode decomposition and Hilbert spectral analysis. EPL (Europhysics Letters). 2008;**84**(4):40010

[39] Ismail DKB, Lazure P, Puillat I. Advanced spectral analysis and cross correlation based on the empirical mode decomposition: Application to the environmental time series. IEEE Geoscience and Remote Sensing Letters. 2015;**12**(9):1968-1972

[40] Li X, Li Z, Wang E, Feng J, Kong X, Chen L, et al. Analysis of natural mineral earthquake and blast based on Hilbert–Huang transform (HHT). Journal of Applied Geophysics. 2016;**128**:79-86

[41] Kader B, Yaglom A. Spectra and correlation functions of surface layer atmospheric turbulence in unstable thermal stratification. In: Turbulence and Coherent Structures. Dordrecht: Springer; 1991. pp. 387-412

[42] Huang Y, Schmitt FG, Hermand JP, Gagne Y, Lu Z, Liu Y, et al. Arbitrary-order Hilbert spectral analysis for time series possessing scaling statistics: Comparison study with detrended fluctuation analysis and wavelet leaders. Physical Review E. 2011;**84**(1):016208

[43] Zhang C, Ni Z, Ni L. Multifractal detrended cross-correlation analysis between PM2.5 and meteorological factors. Physica A: Statistical Mechanics and its Applications. 2015;**438**:114-123

[44] Tchen C. On the spectrum of energy in turbulent shear flow. Journal of Research of the National Bureau of Standards. 1953;**50**:51-62

[45] Katul GG, Porporato A, Nikora V. Existence of k^{-1} power-law scaling in the equilibrium regions of wall-bounded turbulence explained by Heisenberg's eddy viscosity. Physical Review E. 2012;**86**(6):066311

[46] Iatsenko D, McClintock PV, Stefanovska A. Linear and synchrosqueezed time–frequency representations revisited: Overview, standards of use, resolution, reconstruction, concentration, and

algorithms. Digital Signal Processing.
2015;**42**:1-26

[47] Varotsos C, Ondov J, Efstathiou M.
Scaling properties of air pollution in
Athens, Greece and Baltimore,
Maryland. Atmospheric Environment.
2005;**39**(22):4041-4047

[48] Prospero JM, Collard FX, Molinié J,
Jeannot A. Characterizing the annual
cycle of African dust transport to the
Caribbean Basin and South America and
its impact on the environment and air
quality. Global Biogeochemical Cycles.
2014;**28**(7):757-773